Published in final edited form as:
Mech Dev. 2014 August ; 0: 11–22. doi:10.1016/j.mod.2014.07.002.

Hepatocyte Growth Factor-Like Protein is a Positive Regulator of Early Mammary Gland Ductal Morphogenesis

Devikala Gurusamy[1,4], **Sasha J. Ruiz-Torres**[1,4], **Abby L. Johnson**[2,4], **Dana A. Smith**[1], and **Susan E. Waltz**[1,3,*]

[1]Department of Cancer Biology, University of Cincinnati College of Medicine, Cincinnati, OH 45267-0521 USA

[2]Department of Environmental Health, University of Cincinnati College of Medicine, Cincinnati, OH 45267-0521 USA

[3]Research Service, Cincinnati Veterans Hospital Medical Center, Cincinnati, OH 45267-0521 USA

Abstract

The Ron receptor tyrosine kinase regulates multiple cellular processes and is important during mammary gland development and tumor progression. Hepatocyte growth factor-like protein [HGFL] is the only known ligand for the Ron receptor and recent studies have identified major roles for HGFL during breast cancer metastasis. Understanding the functional importance HGFL during mammary gland development will provide significant insights onto its contribution during tumor development and metastasis. In this study, we assessed the role of HGFL during postnatal mammary gland development using mice that were either proficient [HGFL+/+] or deficient [HGFL−/−] for HGFL. Postnatal ductal morphology and stromal cell associations were analyzed at multiple time points through puberty until adulthood. HGFL deficiency resulted in several mammary gland developmental defects including smaller Terminal End Buds [TEBs], significantly fewer TEBs, and delayed ductal outgrowth during early puberty. Additionally, HGFL deficient animals exhibited significantly altered TEB epithelial cell turnover with decreased proliferation and increased apoptosis coupled with decreased TEB diameter. Macrophage recruitment to the TEBs was also significantly decreased in the HGFL−/− mice compared to controls. Moreover, the levels of STAT3 mRNA as well as the phosphorylation status of this protein were lower in the HGFL−/− mammary glands compared to controls. Taken together, our data provide the first evidence for HGFL as a positive regulator of mammary gland ductal morphogenesis by controlling overall epithelial cell turnover, macrophage recruitment, and STAT3 activation in the developing mammary gland. With a function in early mammary gland

*Address Correspondence to: Susan E. Waltz, PhD, University of Cincinnati College of Medicine, Department of Cancer Biology, 3125 Eden Avenue, Cincinnati, OH 45267-0521, Tel: 513-558-8675, Fax: 513-558-4428, susan.waltz@uc.edu.
[4]These authors contributed equally to this work.

development, HGFL represents a potential target for the development of novel breast cancer therapies.

Keywords

HGFL; Ron receptor; cell proliferation; cell apoptosis; macrophages; STAT3; Mammary gland development

1. Introduction

The mammary gland is a complex structure composed of epithelial and stromal cells that include fibroblasts, adipocytes, endothelial cells, nerve cells, and migratory leukocytes [macrophages and eosinophils] (Gouon-Evans et al., 2002). The development of a mammary gland is a highly regulated and intricate process that occurs throughout the life of an animal, beginning in the embryo and continuing postnatally during puberty, pregnancy, lactation, and involution (Richert et al., 2000). During embryonic development, a rudimentary mammary gland ductal structure invades the mesenchymal tissue and remains dormant until approximately 21 days of age, where the onset of ovarian hormone secretions stimulate ductal growth (Richert et al., 2000). Terminal end bud structures [TEB] are found exclusively in the developing mammary gland and are the main driving force for mammary gland development. During puberty, TEB formation and side branching drive mammary gland epithelial cell invasion into the mammary fat pad (Sternlicht, 2006). Additional primary ducts are formed through bifurcation of existing TEBs. Trailing ducts sprout secondary branches, while short tertiary branches form off of the developed secondary branches (McNally and Martin, 2011). This extension of ductal branching into the surrounding fat pad continues until the entire fat pad is filled.

Pubertal mammary gland morphogenesis integrates a balance of epithelial cell proliferation, differentiation, and apoptosis (McNally and Martin, 2011). In addition, several studies have identified the interactions between mammary epithelial cells, mesenchymal cells, and leukocytes to be crucial for the proper postnatal development of the mammary ductal tree (Gouon-Evans et al., 2002; Gouon-Evans et al., 2000; Sternlicht, 2006; Wiseman and Werb, 2002). Interestingly, studies have shown that processes important in mammary gland development are often deregulated during breast cancer tumorigenesis (Lanigan et al., 2007; Micalizzi et al., 2010). Thus, understanding the complex signaling network as well as the interactions between the different cell types during mammary gland development will be vital for elucidating the mechanisms underlying breast cancer progression and metastasis.

Mammary gland development is dependent on many growth factors that target receptor tyrosine kinases, including epidermal growth factor [EGF], insulin-like growth factor [IGF], and hepatocyte growth factor [HGF] (Garner et al., 2011). EGFR, IGFR, and HGFR [also known as c-Met], the tyrosine kinase receptors associated with these growth factors, have also been found to be associated with poor prognosis in breast cancer (Chrysogelos and Dickson, 1994; Lengyel et al., 2005; Resnik et al., 1998). In studies with EGFR impaired kinase activity, a decrease in branching and ductal extension and hence overall mammary gland development was observed compared to wild type controls (Sebastian et al., 1998).

Studies using mice that lacked the IGFR ligand, IGF, showed that mammary gland development was not possible without IGF, suggesting its central role in this process (Ruan and Kleinberg, 1999). Using a conditional deletion of c-Met receptor that inhibited HGF signaling, it was shown that loss of HGF signaling leads to a 35% reduction in overall branching morphogenesis (Garner et al., 2011). Hepatocyte growth factor-like protein [HGFL] shares 45% amino acid homology to HGF (Wagh et al., 2008). Because of the similarities between HGF and HGFL and the established importance of growth factors and their associated receptor tyrosine kinases during mammary gland development, we chose to study the effects of HGFL in this context.

The Ron receptor tyrosine kinase, a member of the c-Met family of receptor tyrosine kinases, is overexpressed in about 50% of primary breast cancers (Wagh et al., 2008). Previously, our laboratory has shown the Ron receptor to be important during both mammary gland development (Meyer et al., 2009) as well as during breast cancer tumorigenesis (McClaine et al., 2010; Peace et al., 2005; Zinser et al., 2006). HGFL, also known as macrophage stimulating protein [MSP], is the only known ligand for Ron (Bezerra et al., 1993; Wang et al., 1994) and was initially identified as a chemotactic protein capable of inducing macrophage shape change, chemotactic migration, and phagocytosis (Leonard and Skeel, 1976). In a recent study, HGFL was also shown to function as a macrophage chemoattractant in a rat kidney inflammatory model (Rampino et al., 2007).

HGFL is predominantly produced by the hepatocytes and is secreted into the bloodstream as an inactive single chain polypeptide precursor, pro-HGFL. Pro-HGFL then works in an endocrine fashion, when locally cleaved by proteases of the coagulation cascade (Leonard and Danilkovitch, 2000; Wang et al., 1994b) or by matriptase expressed on macrophages (Bhatt et al., 2007), to form an active heterodimer. HGFL-dependent Ron activation results in receptor dimerization and trans-autophosphorylation of key tyrosine residues, leading to activation of downstream signaling targets such as STAT3, Akt, MAPK, and β-catenin, which are shown to be important in both mammary gland development and breast cancer tumorigenesis (Wagh et al., 2008). Interestingly, Ron activation has been shown to increase STAT3 phosphorylation (Danilkovitch-Miagkova, 2003; Gurusamy et al., 2013) and mammary epithelial-specific STAT3 activation has been shown to regulate the number of macrophages recruited to the developing mammary gland (Hughes et al., 2012). Furthermore, STAT3 in macrophages has been shown to regulate the production of inflammatory cytokines and ultimately the tissue microenvironment (Akira, 2000). Interestingly, the coordinated expression of Ron, HGFL, and the protease matriptase has been shown to be a strong independent indicator of both metastasis and poor prognosis in breast cancer patients (Welm et al., 2007). In addition, HGFL expression by tumor cells has been shown to increase the spectrum of metastasis using an orthotopic mouse model of breast cancer (Welm et al., 2007).

Although the Ron receptor was previously shown to be a critical negative regulator of mammary gland ductal morphogenesis (Meyer et al., 2009), the importance of HGFL during mammary gland development was not assessed. In this study, we hypothesized that loss of HGFL will augment mammary gland ductal morphogenesis, similar to the phenotype observed with Ron loss. Our data reported here documents HGFL expression in both the

epithelial and stromal compartments of a developing mammary gland. Interestingly, we found that lack of HGFL expression delayed early mammary gland ductal growth at puberty and is associated with decreased cell proliferation and increased cell apoptosis in the TEBs as well as with decreased macrophage association within the epithelial and stromal cells surrounding the TEBs. Taken together, our studies indicate that HGFL mediated signaling is important for early mammary gland ductal morphogenesis, for proper epithelial cell turnover, and for the recruitment of macrophages to the developing mammary gland.

2. Results

2.1 HGFL is expressed in both epithelial and stromal cell compartments during mammary gland development

To examine the importance of HGFL in mammary gland development, the expression of HGFL was characterized in whole mammary glands during early development. Similar levels of HGFL mRNA expression were observed in wild type [HGFL+/+] mammary glands at 3, 5, and 7 weeks of age [Figure 1A]. The subcellular expression pattern of HGFL was further determined in isolated fractions of epithelial cells, mature adipocytes, and macrophages by qRT-PCR. HGFL expression was detected in the various cellular compartments isolated from HGFL+/+ mammary glands, including the epithelial cells and macrophages and, to a lesser extent, in mature adipocytes [Figure 1B]. Immunohistochemical detection of HGFL in wild type mammary glands showed staining in both the epithelial and stromal compartments with specificity of staining confirmed with the use of a HGFL-specific blocking peptide [Figure 1C]. Furthermore, the expression of Ron receptor was not different between HGFL+/+ and HGFL−/− glands at 3, 5, and 7 weeks of age, suggesting that receptor expression is not altered to compensate for the loss of ligand [Figure 1D]. Overall, our data demonstrate that HGFL is expressed in both the epithelial and stromal cell compartments during mammary gland development and that HGFL deficiency does not alter Ron expression in the developing mammary gland.

2.2 HGFL deficiency delays early postnatal mammary gland development

To determine the functional significance of HGFL during mammary gland development, the growth patterns of HGFL+/+ and HGFL−/− mammary glands were examined at multiple developmental time points, ranging from 3, 4, 5, 6, 7, 8 to 10 weeks of age. HGFL−/− mammary glands exhibited significantly stunted ductal outgrowth during the juvenile [3 weeks] and pubertal time points [4–5 weeks]. However, by adulthood, ductal outgrowth of HGFL−/− glands equalized to that observed in HGFL+/+ glands, occupying similar regions of the fat pad [Figure 2A and 2C (Richert et al., 2000)]. Accordingly, the primary ductal length, measured from the base of the nipple to the furthest TEB for 3–4 week old mice, showed a significant reduction in the HGFL−/− mammary glands compared to controls [Figure 2B]. Analogous to the ductal outgrowth observed at 3–4 weeks of age, primary ductal length past the lymph node was reduced in HGFL−/− mammary glands at 5 weeks of age when compared to controls [Figure 2C]. During the mid-to-late stage of pubertal mammary development [6–10 weeks], the primary ductal length past the lymph node was similar between HGFL+/+ and HGFL−/− mammary glands [Figure 2C]. Overall, these results suggest that HGFL is not necessary for the establishment of the rudimentary ductal

tree during the neonatal period, but mediates ductal outgrowth during puberty until adulthood, at which point HGFL−/− glands reach full outgrowth similar to HGFL proficient counterparts.

To further evaluate developmental progress, we measured the diameter of TEBs, the number of TEBs, and branching morphogenesis in HGFL+/+ and HGFL−/− mammary glands. Interestingly, decreases in TEB diameter were observed in pubertal HGFL−/− mammary glands when compared to control counterparts, suggesting that HGFL deficiency reduces the number of epithelial cells in the TEB [Figure 3A]. In addition, mammary glands from HGFL −/− mice exhibited a significant decrease in the number of TEBs at 3 weeks of age when compared to HGFL+/+ controls [Figure 3B]. No significant differences were observed in the formation of secondary and tertiary structures from the primary duct throughout postnatal development until adulthood [Figure 3C and 3D]. These data suggest that HGFL deficiency delays early mammary gland ductal morphogenesis, while mammary gland branching morphogenesis remains unaltered in the absence of HGFL.

2.3 Normal mammary gland epithelial cell turnover depends on HGFL

Normal postnatal mammary gland development is balanced by periodic proliferation of the TEB epithelial cells and removal of TEB epithelial cells by physiological cell death (Strange et al., 2001). As TEB size was significantly smaller in HGFL−/− mammary glands compared to wild type controls throughout puberty, we sought to determine if HGFL partakes in the regulation of epithelial cell proliferation and/or cell death within TEBs. We performed Ki67 and TUNEL analysis, respectively, on the isolated HGFL+/+ and HGFL−/− mammary glands at 3, 5, and 7 weeks of age [Figure 4A and 4C]. The number of Ki67 positive or TUNEL positive cells within the TEBs between the two genetic groups was counted as the percentage of positively stained cells to the total number of cells in the TEBs. The data are represented as an average of the percentage of positive cells per group [Figure 4B and 4D]. A significant decrease in epithelial cell proliferation was observed in the HGFL −/− TEBs compared to controls [Figure 4A and 4B]. Additionally, a significant increase in epithelial cell death was observed in HGFL−/− mammary gland TEBs compared to controls [Figure 4C and 4D]. Overall, these results suggest that HGFL ablation delays early postnatal mammary gland development, in part, by altering the overall epithelial cell turnover in the TEB of the mammary gland.

2.4 HGFL−/− mammary glands have fewer macrophages surrounding TEBs of the developing mammary gland compared to HGFL+/+ glands

We next sought to determine if alterations in macrophages might contribute to the diminished development of the epithelial ductal tree in HGFL−/− mammary glands. Interactions between epithelial cells and macrophages in the TEBs have been shown to play a major role in tissue remodeling during mammary gland development by regulating TEB formation, TEB outgrowth, and the branching of the associated ducts (Gouon-Evans et al., 2000). F4/80 immunohistochemical staining for macrophages was performed on 3, 5, and 7 week HGFL+/+ and HGFL −/− mammary glands [Figure 5A]. The number of macrophages within the TEBs as well as the surrounding stromal region was determined and is depicted in Figure 5B and 5C. The number of macrophages recruited to both the stroma surrounding the

TEBs as well as within the TEBs was significantly lower in HGFL−/− mammary glands compared to HGFL+/+ [Figure 5B and 5C]. Consistent with this finding, qRT-PCR analysis of F4/80 in mammary glands from 7-week mice revealed decreased expression of F4/80 in the HGFL−/− glands when compared to the HGFL+/+ controls [Figure 5D]. These data demonstrate that HGFL deficiency leads to decreased recruitment of macrophages within and around the TEBs of the developing mammary gland, suggesting that HGFL regulates ductal extension throughout puberty by controlling macrophage recruitment during development. qRT-PCR analysis was also performed from glands at 7 weeks to identify signaling differences between HGFL+/+ and HGFL−/− mammary glands that may influence macrophage recruitment. The expression of the monocyte recruitment chemokines, monocyte chemoattractant protein-1 [MCP-1] and Interleukin 6 [IL-6], were significantly reduced in HGFL−/− mammary glands when compared to the HGFL+/+ glands [Figure 5E]. Furthermore, the receptor for MCP-1, C–C chemokine receptor type 2 [CCR-2], also exhibited significantly reduced mRNA expression in HGFL−/− mammary glands compared to age-matched controls [Figure 5E]. Together, our data suggest that HGFL ablation alters macrophage recruitment to the mammary gland by regulating chemoattractant expression.

2.5 HGFL-mediated Ron signaling in the mammary gland is associated with increased STAT3 mRNA expression and phosphorylation status

Given that Ron is upstream of STAT3 and that STAT3 expression in mammary epithelial cells can promote macrophage recruitment to the mammary gland (Hughes et al., 2012) and regulate MCP-1 expression (Potula et al., 2009), the expression of STAT3 was characterized in HGFL+/+ and HGFL−/− mammary glands. The expression of STAT3 mRNA was significantly reduced in HGFL−/− mammary glands compared to controls [Figure 6A]. However, Western analysis did not detect differences in the levels of the total protein between groups [Figure 6B]. Interestingly, the levels of the phosphorylated STAT3 protein [pSTAT3] were significantly different between groups, with increased pSTAT3 detected in the HGFL+/+ mammary glands compared to HGFL−/− glands [Figure 6B]. To determine the cell type specification of pSTAT3 in the mammary gland tissue, immunohistochemical staining of pSTAT3 was performed on mammary glands from HGFL+/+ and HGFL−/− animals [Figure 6C]. The expression of pSTAT3 was primarily restricted to the epithelial cells of the TEB, as shown in Figure 6C. Quantification of the percent of pSTAT3 positive cells showed a significant decrease in pSTAT3 positive epithelial cells in HGFL−/− TEBs compared to the HGFL+/+ mice and a significant decrease in pSTAT3 in HGFL−/− surrounding stromal cells compared to controls [Figure 6C]. Overall, our results suggest that HGFL-dependent Ron signaling within mammary epithelial and stromal cells regulates STAT3 signaling and is correlated with increases in macrophage recruitment and ductal extension [Figure 6C].

3. Discussion

The ability of the mammary gland to undergo normal development and proper lobulo-alveolar remodeling during pregnancy is critical for the reproductive health of an animal. Mammary gland development is a highly regulated process distinct from the development of other organs, since much of the ductal and branching morphogenesis occurs postnatally with

the onset of puberty rather than in utero (LaRocca et al., 2011). Among the many factors involved in mammary gland development, a number of receptor tyrosine kinases and their associated ligands have been shown to play important roles. Most importantly, the receptors of these ligands have been shown to be factors important in breast tumorigenesis.

The Ron receptor and its only known ligand, HGFL, have been strongly correlated as prognostic indicators of breast cancer progression and metastasis, associated with poor patient outcome (Maggiora et al., 1998; Welm et al., 2007). Previous studies from our laboratory investigating the role of the Ron receptor tyrosine kinase in mammary gland development showed that loss of Ron signaling in mice resulted in increased ductal extension at 6 and 7 weeks of age and increased secondary and tertiary branching at 6, 7, and 8 weeks of age when compared to Ron expressing control mice (Meyer et al., 2009). Since HGFL is the only known ligand for the Ron receptor, we investigated whether HGFL-dependent Ron activation affects ductal and branching morphogenesis during mammary gland development. Using the HGFL+/+ and HGFL−/− mice, we found that HGFL was important for proper mammary gland organogenesis, with the initial formation of the rudimentary ductal tree during embryonic development being HGFL-independent. Our study also showed that HGFL affected postnatal development by regulating mammary gland ductal extension as well as the number of TEBs present at the onset of puberty. The role of HGFL as a positive regulator of mammary gland development is characteristic of information that has been shown with other growth factors, such as EGF (Sebastian et al., 1998) and HGF (Garner et al., 2011).

Interestingly, the results obtained from the HGFL−/− animals do not coincide with those examining Ron receptor loss during mammary gland development, wherein Ron loss led to exaggerated branching morphogenesis (Meyer et al., 2009). Given that the Ron receptor is capable of crosstalk with other receptor tyrosine kinases, like c-MET and EGFR, in the presence or absence of HGFL, loss of the Ron ligand may be less detrimental for mammary gland development compared to Ron receptor loss (Danilkovitch-Miagkova and Leonard, 2001; Follenzi et al., 2000; McCleese et al., 2013). In HGFL deficient mice, Ron transactivation through heterodimerization with other receptor tyrosine kinases [RTKs] may be operant (Meyer et al., 2009). Furthermore, different mutations in the tyrosine kinase domain of RTKs have been shown to generate biologically distinct phenotypes (Grundler et al., 2005), further supporting the complex mechanisms through which RTKs can signal. Our data presented in this paper show the importance of HGFL signaling through an intact Ron receptor, suggestive that the ligand dependent activation of Ron promotes mammary gland development. However, the functional differences observed in the ligand dependent and independent roles of the Ron receptor as well as the differences in tyrosine kinase signaling during mammary gland development warrants further investigation.

Pro-HGFL is produced by the hepatocytes and released into the circulation, where it is cleaved and activated locally at target sites. Localized expression of HGFL in the various stromal and epithelial cells of the mammary gland was detected at the level of both mRNA and protein [Figure 1B and **1C**], suggestive of potential autocrine and paracrine signaling roles of the ligand during mammary gland development. This is important, since recent

studies have linked autocrine secretion of HGFL to lung and breast tumor metastasis (Sato et al., 2013; Welm et al., 2007).

Mammary gland postnatal development depends upon both periodic proliferation and removal of mammary epithelial cells (Strange et al., 2001). Our study showed that HGFL ablation decreased epithelial cell proliferation and increased epithelial cell death in the TEB concomitant with decreased TEB size, illustrating the importance of HGFL in proper mammary epithelial cell growth and mammary gland development. In addition to mammary epithelial growth, proper postnatal mammary gland development also relies on the functions of several stromal cell types, including fibroblasts, adipocytes, and inflammatory infiltrates (Gouon-Evans et al., 2002; Wiseman and Werb, 2002). A major inflammatory cell type infiltrating the mammary glands is the macrophage, which has been shown to play important roles during ductal elongation and branching (Gouon-Evans et al., 2002). Previous studies using different inflammatory model systems have shown HGFL to be a monocyte/macrophage chemoattractant to injured tissues (Nanney et al., 1998; Rampino et al., 2007). In our model system, we observed a significant decrease in the mRNA expression levels of the monocyte chemoattractant MCP-1 and its receptor, CCR-2, in mammary glands isolated from HGFL−/− mice [Figure 5E]. Similarly, IL-6 mRNA levels were also significantly reduced in HGFL−/− mammary glands. Furthermore, the number of macrophages infiltrating the HGFL−/− mammary glands was significantly reduced compared to the controls [Figure 5A, 5B, and **5C**]. These data collectively emphasize the importance of HGFL as a macrophage chemoattractant to the TEBs of the developing mammary gland that may then promote the ductal extension as well as the proliferation, maintenance, and/or differentiation of the mammary gland (Gouon-Evans et al., 2000; Hughes et al., 2012; Sternlicht, 2006).

Studies have shown that MCP-1 gene expression is regulated in a STAT3-dependent manner (Potula et al., 2009). Interestingly, in our model we observed a significant reduction in the levels of pSTAT3 in both epithelial cells of TEBs and surrounding stromal cells of the HGFL−/− mammary glands compared to the controls [Figure 6C]. The expression of pSTAT3 was primarily restricted to the epithelial cells of the TEBs. Previous studies on mice containing epithelial specific STAT3 deletions have shown STAT3 to have effects on the inflammatory signature of the mammary gland as well as on the polarization of the macrophages to an alternatively activated phenotype during mammary gland involution (Hughes et al., 2012). In macrophages, STAT3 has been shown to be responsible for stimulating anti-inflammatory responses, thus regulating the tissue microenvironment (Akira, 2000). This is significant as a recent study in a cancer system demonstrated that Ron expression in tumor-associated-macrophages promotes alternative macrophage [M2] activation and represses the activity of cytotoxic CD8+ T cells, driving tumorigenesis in an immunosuppressive microenvironment through increased activation of STAT3 (Gurusamy et al., 2013). Furthermore, STAT-3 activation in breast cancer is predominantly mediated through the actions of IL-6 (Berishaj et al., 2007), which was reduced in the developing mammary gland with loss of HGFL [Figure 5E]. Additional Ron downstream signaling pathways were examined in the HGFL−/− mouse model. However, MAPK, β-catenin, and Akt protein expression in the mammary gland were not altered with loss of HGFL during

puberty (data not shown). These prior studies and our results support the contention that the epithelial and stromal cell-type specific HGFL-mediated Ron activation promotes the phosphorylation of STAT3 and subsequently influences the number of macrophages recruited to the developing mammary gland. The importance of HGFL-mediated regulation of STAT3 activation and macrophage recruitment during pregnancy, lactation, and involution and tumorigenesis has yet to be evaluated.

Taken together, the results reported herein provide the fundamental importance of HGFL in normal mammary gland development that may be extended to understand mammary tumorigenesis. An important phenotype observed in these studies, which would be vital for understanding mammary tumorigenesis, is the influence of HGFL on the number of TEBs observed at the onset of puberty. The TEBs are structures shown to contain a special population of pluripotent stem cells, which ultimately differentiate to form the various cell layers of the epithelial duct (Smalley and Ashworth, 2003). The TEBs are permanently replaced with terminal ducts and alveolar buds in the adult gland. However, the adult gland has been reported to retain the mammary gland stem cell population capable of giving rise to epithelial precursor cells (Ball, 1998). Evaluation of the role of HGFL on regulating the number of TEBs as well as the stem cell pluripotency and differentiation will aid in understanding its role during breast tumor initiation and progression. In conclusion, we have shown HGFL to be a positive regulator of mammary gland development by controlling ductal extension through both the epithelial cell turnover and the STAT3-mediated macrophage recruitment to the developing mammary gland.

4. Experimental Procedures

4.1 Animals

HGFL−/− mice have been previously described (Bezerra et al., 1998). The animals were backcrossed 8 generations onto the FVB/N background for studies described herein. Age matched FVB/N mice were used as wild-type controls for all our experiments. All experiments involving animals were performed under protocols approved by the Institutional Animals and Use Committee of the University of Cincinnati.

4.2 Whole mount and histological analyses

Mammary glands from 3, 4, 5, 6, 7, 8, and 10-week-old virgin female HGFL+/+ and HGFL −/− mice [n=6–18 per genotype] were harvested. One inguinal gland was prepared for whole mount morphological analysis, while another inguinal gland was fixed in formalin and processed for paraffin sectioning and histology. The thoracic glands were frozen for RNA and protein analysis. For whole mount preparation, glands were spread on glass slides and fixed overnight in Carnoy's fixative, then hydrated in graded series of ethanol before being stained overnight with Carmine Alum (Meyer et al., 2009). After staining, glands were dehydrated in a graded series of ethanol and then cleared in Xylene before mounting with Permount [Thermo Fisher Scientific, Waltham, MA, USA]. Whole mount images were taken with a Leica DFC295 camera [Leica Microsystems Ltd., Buffalo Grove, IL, USA] on a Leica KL-200 LED stereoscope [Leica Microsystems Ltd.] and ductal elongation measured using Image Pro Insight Software [Media Cybernetics, Rockville, MD, USA]. For

histological analysis, the glands were fixed overnight in 10% neutral buffered formalin, then switched to 70% ethanol, processed, and embedded in paraffin. Histological images were taken with a Zeiss AxioCam MRc5 camera attached to an Olympus BX41 microscope [Olympus, Center Valley, PA, USA] using the Axiovision Rel. 4.8 software [Carl Zeiss MicroImaging, GmbH, Germany].

4.3 Immunohistochemistry

Formalin fixed and paraffin embedded mammary glands sectioned at 4μm thickness were used for immunohistochemical staining of HGFL [Santa Cruz Biotechnology, Texas, USA], HGFL blocking peptide [Santa Cruz Biotechnology], pSTAT3 Y-705 [Cell Signaling, Danvers, MA, USA], Ki67 [Thermo Fisher Scientific, Waltham, MA, USA], and F4/80 [eBiosciences, San Diego, USA]. The tissue sections were deparaffinized and rehydrated with antigen retrieval carried out using citrate buffer [HGFL, Ki67, and pSTAT3] or proteinase K [F4/80], depending on the nature of the antigen being detected. The sections were blocked for endogenous peroxidase activity by incubating in 0.5% hydrogen peroxide in methanol for 15 minutes. After blocking for non-specific binding sites using 10% normal serum solution for an hour at RT, the tissue sections were incubated in primary antibody overnight at 4°C. The slides were washed in 1X PBS and labeled with biotinylated secondary antibody [Vector Laboratories, Burlingame, CA]. The tissues were then incubated with prepared ABC solution [Vector Laboratories, Burlingame, CA] for 30 minutes. The sections were developed for brown color using 3–3'-diaminobenzidine substrate [Sigma, St. Louis, MO, USA]. The stained sections were counterstained with Heamatoxylin, dehydrated, and mounted. Images of 2–7 fields per section were captured using the Zeiss AxioCam MRc5 camera attached to an Olympus BX41 microscope [Olympus, Center Valley, PA, USA] and Axiovision Rel. 4.8 software [Carl Zeiss MicroImaging, GmbH, Germany]. The number of Ki67, pSTAT3, and F4/80 positive cells between the two genetic groups was counted per field [TEB], the percentage of positive cells to the total number of cells was quantified, and the data was represented as the average percentage of positive cells per TEB per group.

For TUNEL analyses, the rate of cell death in the HGFL+/+ and HGFL−/− mammary gland sections was detected using the Apoptag Plus Peroxidase In-situ Apoptosis kit per manufacturer's instructions [Millipore, Billerica, MA, USA]. Images of 2–5 fields per section were captured as above. The number of TUNEL positive cells between the two genetic groups was counted per field [TEB], the percentage of positive cells to the total number of cells in the TEB was quantified, and the data was represented as the average percentage of positive cells per TEB per group.

4.4 Ductal extension, terminal end buds [TEBs], and branch quantification

Whole mount images of 3, 4, 5, 6, 7, 8, and 10-week-old HGFL+/+ and HGFL−/− inguinal mammary glands were obtained using a Leica DFC295 camera [Leica Microsystems Ltd.] on a Leica KL-200 LED stereoscope [Leica Microsystems Ltd.] and Image Pro Insight Software [Media Cybernetics, Rockville, MD, USA]. Using the Image Pro Insight software, ductal extension was measured starting from the center of the lymph node to the furthest TEB at the leading edge of the mammary epithelium for 5, 6, 7, 8, and 10 week old inguinal

mammary glands, while ductal extension in 3 and 4 week old inguinal mammary glands was measured from the base of the nipple to the furthest TEB at the leading edge of the mammary epithelium. Mammary whole mount images were used to measure the terminal end bud diameters of the two genetic groups using Axiovision Rel. 4.8 software and ImageJ software [ImageJ 1.44p, National Institute of Health, USA], and the data was represented as the mean TEB diameter in micrometers. The number of terminal end buds of the two genetic groups was counted using the ImageJ software. For branch quantification, the longest primary duct above the lymph node was used to count the number of secondary and tertiary branches. A secondary branch was defined as any branch that bifurcates off this primary duct, while a tertiary branch was defined as any branch that bifurcates off of the secondary branches that extend from this primary duct.

4.5 Primary mammary cell isolations

A single-cell suspension of freshly isolated explants of combined inguin*al* and thoracic mammary glands from 5-week-old HGFL+/+ or HGFL−/− mice [n=4 in each group] were obtained by mechanical dissociation and enzymatic digestion with collagenase IV. The digestion was carried out on a magnetic stirrer at 37°C for 2 hours. The cell suspension was then used for the isolation of the mature adipocytes, epithelial, and immune cell fractions using differential centrifugation and antibody coated magnetic beads. For mature adipocyte isolation, the single cell suspension was centrifuged at 1000rpm for 5 minutes at 4°C and the top layer containing the mature adipocytes was skimmed and collected for RNA isolation. The remaining single cell suspension enriched for the epithelial and stromal cellular fractions was centrifuged at 120 x g for 5 minutes at 4°C. The supernatants from the spin were enriched for the immune cells while the pellet contained the epithelial and fibroblastic cells. The supernatant was collected and centrifuged at 800 × g for 11 minutes at 4°C to pellet the tumor-infiltrating immune cell fraction. The pelleted cells were then resuspended in plain RPMI media and subsequently utilized for macrophage isolation using CD11b magnetic beads per manufacturer's instructions [Miltenyi Biotec GmbH, Bergisch Gladbach, Germany] and collected for RNA isolation. For isolation of epithelial cells, the pelleted cells obtained from the 120g spin were resuspended in 1X PBS and pulse spun at 1200rpm for 15s, the supernatant was collected, and the spins were repeated for an additional 3 times. The pellet at the end of the pulse spins contained the epithelial cells.

4.6 Western analyses

Thoracic mammary glands from 3 week old HGFL+/+ and HGFL−/− mice were homogenized in RIPA buffer [20 mM Tris-HCl, pH 7.4, 37 mM NaCl, 2 mM EDTA, 1% Triton X-100, 10% Glycerol, 0.1% SDS, 0.5% Sodium deoxycholate in 1X PBS] supplemented with protease inhibitors [Complete tablets, Roche, Indianapolis, IN, USA] and phosphatase inhibitors [Sodium orthovanadate, Sigma Aldrich, St. Louis, MO, USA]. The samples were then centrifuged at 14,000rpm for 10 min at 4°C and the supernatant collected. Western analysis was performed as previously described (Meyer et al., 2010) using anti-phospho-STAT3 Y-705 and total STAT3 from Cell Signaling Technology [Danvers, MA, USA] and anti-C4 actin antibody [CCHMC, Cincinnati, USA]. To detect primary antibodies, peroxidase-conjugated anti-mouse or anti-rabbit secondary antibodies [Jackson

ImmunoResearch, West Grove, PA, USA] were used. Secondary antibody detection was performed using the Pierce ECL Kit [Pierce Biotechnology, Rockford, IL, USA].

4.7 Quantitative real time PCR [qRT-PCR] analysis

RNA was isolated from whole glands, purified epithelial cells, macrophages, and mature adipocytes using the TRIZOL method. Purified RNA was placed in a cDNA reaction using the high capacity cDNA kit [Applied Biosystems, Foster City, CA, USA] according to manufacturer's instructions. The following primer pairs were used for the measurement of transcript levels: mHGFL: 5'-TGGAAAGGGTGCGAGT-3' and 5'-GCTGTGGCATCAAAACCT-3'; mSTAT3 5′;-GAA GACCAAGTTCATCTGTGTG-3′; and 5′-GTAGCACACTCCGAGGTCAGAT-3′; mMCP-1 5'-GCCCCACTCACCTGCTGCTA-3' and 5'-TTTACGGGTCAACTTCACATTCAA-3'; mRON 5'-TCCCATTGCAGGTCTGTGTAGA-3' and 5'-CGGAAGCTGTATCGTTGATGTC-3'; F4/80 5'-GAGATTGTGGAAGCATCCGAGAC-3' and 5'-GATGACTGTACCCACATGGCTGA-3'; mIL-6 5'-TTGGTCCTTAGCCACTCCTTC-3' and 5'-TAGTCCTTCCTACCCCAATTTCC-3'; mCCR-2 5'-AGCACATGTGGTGAATCCAA-3' and 5'-TGCCATCATAAAGGAGCCA-3'; and mGUS 5'-TTGAGAACTGGTATAAGACGCATCAG-3' and 5'-TCTGGTACTCCTCACTGAACATGC-3', which was used as an internal control. Relative gene expression normalized to the internal control is reported.

4.8 Statistical analyses

All data was represented as the mean of the samples ± Standard Error of the Mean [SEM]. Statistical significance was determined by Student's *t* -test using GraphPad Prism [GraphPad Software, San Diego, CA, USA]. $P<0.05$ was considered significant for all analyses.

Acknowledgments

The authors would like to thank Glenn Doerman, Madison Nashu, Juozas Vasiliauskas and Jerilyn Gray for their excellent technical assistance. This work was supported by grant 1IOBX000803 from the Cincinnati Veteran's Medical Center and by T32 CA117846-05 from the National Institute of Health.

References

Akira S. Roles of STAT3 defined by tissue-specific gene targeting. Oncogene. 2000; 19:2607–2611. [PubMed: 10851059]

Ball SM. The development of the terminal end bud in the prepubertal-pubertal mouse mammary gland. Anat Rec. 1998; 250:459–464. [PubMed: 9566536]

Berishaj M, Gao SP, Ahmed S, Leslie K, Al-Ahmadie H, Gerald WL, Bornmann W, Bromberg JF. Stat3 is tyrosine-phosphorylated through the interleukin-6/glycoprotein 130/Janus kinase pathway in breast cancer. Breast Cancer Res. 2007; 9:R32. [PubMed: 17531096]

Bezerra JA, Carrick TL, Degen JL, Witte D, Degen SJ. Biological effects of targeted inactivation of hepatocyte growth factor-like protein in mice. J Clin Invest. 1998; 101:1175–1183. [PubMed: 9486989]

Bezerra JA, Han S, Danton MJ, Degen SJ. Are hepatocyte growth factor-like protein and macrophage stimulating protein the same protein? Protein Sci. 1993; 2:666–668. [PubMed: 8518737]

Bhatt AS, Welm A, Farady CJ, Vasquez M, Wilson K, Craik CS. Coordinate expression and functional profiling identify an extracellular proteolytic signaling pathway. Proc Natl Acad Sci U S A. 2007; 104:5771–5776. [PubMed: 17389401]

Chrysogelos SA, Dickson RB. EGF receptor expression, regulation, and function in breast cancer. Breast Cancer Res Treat. 1994; 29:29–40. [PubMed: 8018962]

Danilkovitch-Miagkova A. Oncogenic signaling pathways activated by RON receptor tyrosine kinase. Curr Cancer Drug Targets. 2003; 3:31–40. [PubMed: 12570659]

Danilkovitch-Miagkova A, Leonard EJ. Cross-talk between RON receptor tyrosine kinase and other transmembrane receptors. Histol Histopathol. 2001; 16:623–631. [PubMed: 11332718]

Follenzi A, Bakovic S, Gual P, Stella MC, Longati P, Comoglio PM. Crosstalk between the proto-oncogenes Met and Ron. Oncogene. 2000; 19:3041–3049. [PubMed: 10871856]

Garner OB, Bush KT, Nigam KB, Yamaguchi Y, Xu D, Esko JD, Nigam SK. Stage-dependent regulation of mammary ductal branching by heparan sulfate and HGF-cMet signaling. Dev Biol. 2011; 355:394–403. [PubMed: 21586278]

Gouon-Evans V, Lin EY, Pollard JW. Requirement of macrophages and eosinophils and their cytokines/chemokines for mammary gland development. Breast cancer research : BCR. 2002; 4:155–164. [PubMed: 12100741]

Gouon-Evans V, Rothenberg ME, Pollard JW. Postnatal mammary gland development requires macrophages and eosinophils. Development. 2000; 127:2269–2282. [PubMed: 10804170]

Grundler R, Miething C, Thiede C, Peschel C, Duyster J. FLT3-ITD and tyrosine kinase domain mutants induce 2 distinct phenotypes in a murine bone marrow transplantation model. Blood. 2005; 105:4792–4799. [PubMed: 15718420]

Gurusamy D, Gray JK, Pathrose P, Kulkarni RM, Finkleman FD, Waltz SE. Myeloid-specific expression of Ron receptor kinase promotes prostate tumor growth. Cancer research. 2013; 73:1752–1763. [PubMed: 23328584]

Hughes K, Wickenden JA, Allen JE, Watson CJ. Conditional deletion of Stat3 in mammary epithelium impairs the acute phase response and modulates immune cell numbers during post-lactational regression. The Journal of pathology. 2012; 227:106–117. [PubMed: 22081431]

Lanigan F, O'Connor D, Martin F, Gallagher WM. Molecular links between mammary gland development and breast cancer. Cell Mol Life Sci. 2007; 64:3159–3184. [PubMed: 17955178]

LaRocca J, Pietruska J, Hixon M. Akt1 Is Essential for Postnatal Mammary Gland Development, Function, and the Expression of Btn1 a1. PLoS ONE. 2011; 6:1–11.

Lengyel E, Prechtel D, Resau JH, Gauger K, Welk A, Lindemann K, Salanti G, Richter T, Knudsen B, Vande Woude GF, Harbeck N. C-Met overexpression in node-positive breast cancer identifies patients with poor clinical outcome independent of Her2/neu. Int J Cancer. 2005; 113:678–682. [PubMed: 15455388]

Leonard EJ, Danilkovitch A. Macrophage stimulating protein. Adv Cancer Res. 2000; 77:139–167. [PubMed: 10549357]

Leonard EJ, Skeel A. A serum protein that stimulates macrophage movement, chemotaxis and spreading. Experimental cell research. 1976; 102:434–438. [PubMed: 976357]

Maggiora P, Marchio S, Stella MC, Giai M, Belfiore A, De Bortoli M, Di Renzo MF, Costantino A, Sismondi P, Comoglio PM. Overexpression of the RON gene in human breast carcinoma. Oncogene. 1998; 16:2927–2933. [PubMed: 9671413]

McClaine RJ, Marshall AM, Wagh PK, Waltz SE. Ron receptor tyrosine kinase activation confers resistance to tamoxifen in breast cancer cell lines. Neoplasia. 2010; 12:650–658. [PubMed: 20689759]

McCleese JK, Bear MD, Kulp SK, Mazcko C, Khanna C, London CA. Met interacts with EGFR and Ron in canine osteosarcoma. Vet Comp Oncol. 2013; 11:124–139. [PubMed: 22235915]

McNally S, Martin F. Molecular regulators of pubertal mammary gland development. Ann Med. 2011; 43:212–234. [PubMed: 21417804]

Meyer SE, Peace BE, Bahassi el M, Kavanaugh GM, Wagh PK, Robbins SB, Yin M, Wells SI, Zinser GM, Stambrook PJ, Waltz SE. Chk2*1100delC Acts in synergy with the Ron receptor tyrosine kinase to accelerate mammary tumorigenesis in mice. Cancer Lett. 2010; 296:186–193. [PubMed: 20434834]

Meyer SE, Zinser GM, Stuart WD, Pathrose P, Waltz SE. The Ron receptor tyrosine kinase negatively regulates mammary gland branching morphogenesis. Dev Biol. 2009; 333:173–185. [PubMed: 19576199]

Micalizzi DS, Farabaugh SM, Ford HL. Epithelial-mesenchymal transition in cancer: parallels between normal development and tumor progression. Journal of mammary gland biology and neoplasia. 2010; 15:117–134. [PubMed: 20490631]

Nanney LB, Skeel A, Luan J, Polis S, Richmond A, Wang MH, Leonard EJ. Proteolytic cleavage and activation of pro-macrophage-stimulating protein and upregulation of its receptor in tissue injury. J Invest Dermatol. 1998; 111:573–581. [PubMed: 9764835]

Peace BE, Toney-Earley K, Collins MH, Waltz SE. Ron receptor signaling augments mammary tumor formation and metastasis in a murine model of breast cancer. Cancer Res. 2005; 65:1285–1293. [PubMed: 15735014]

Potula HS, Wang D, Quyen DV, Singh NK, Kundumani-Sridharan V, Karpurapu M, Park EA, Glasgow WC, Rao GN. Src-dependent STAT-3-mediated expression of monocyte chemoattractant protein-1 is required for 15(S)-hydroxyeicosatetraenoic acid-induced vascular smooth muscle cell migration. J Biol Chem. 2009; 284:31142–31155. [PubMed: 19736311]

Rampino T, Soccio G, Gregorini M, Guidetti C, Marasa M, Maggio M, Panichi V, Migliori M, Libetta C, Dal Canton A. Neutralization of macrophage-stimulating protein ameliorates renal injury in anti-thy 1 glomerulonephritis. J Am Soc Nephrol. 2007; 18:1486–1496. [PubMed: 17409315]

Resnik JL, Reichart DB, Huey K, Webster NJ, Seely BL. Elevated insulin-like growth factor I receptor autophosphorylation and kinase activity in human breast cancer. Cancer Res. 1998; 58:1159–1164. [PubMed: 9515800]

Richert MM, Schwertfeger KL, Ryder JW, Anderson SM. An atlas of mouse mammary gland development. Journal of mammary gland biology and neoplasia. 2000; 5:227–241. [PubMed: 11149575]

Ruan W, Kleinberg DL. Insulin-like growth factor I is essential for terminal end bud formation and ductal morphogenesis during mammary development. Endocrinology. 1999; 140:5075–5081. [PubMed: 10537134]

Sato S, Hanibuchi M, Kuramoto T, Yamamori N, Goto H, Ogawa H, Mitsuhashi A, Van TT, Kakiuchi S, Akiyama S, Nishioka Y, Sone S. Macrophage stimulating protein promotes liver metastases of small cell lung cancer cells by affecting the organ microenvironment. Clinical & experimental metastasis. 2013; 30:333–344. [PubMed: 23011677]

Sebastian J, Richards RG, Walker MP, Wiesen JF, Werb Z, Derynck R, Hom YK, Cunha GR, DiAugustine RP. Activation and function of the epidermal growth factor receptor and erbB-2 during mammary gland morphogenesis. Cell Growth Differ. 1998; 9:777–785. [PubMed: 9751121]

Smalley M, Ashworth A. Stem cells and breast cancer: A field in transit. Nature reviews. Cancer. 2003; 3:832–844. [PubMed: 14668814]

Sternlicht MD. Key stages in mammary gland development: the cues that regulate ductal branching morphogenesis. Breast Cancer Res. 2006; 8:201. [PubMed: 16524451]

Strange R, Metcalfe T, Thackray L, Dang M. Apoptosis in normal and neoplastic mammary gland development. Microsc Res Tech. 2001; 52:171–181. [PubMed: 11169865]

Wagh PK, Peace BE, Waltz SE. Met-related receptor tyrosine kinase Ron in tumor growth and metastasis. Adv Cancer Res. 2008; 100:1–33. [PubMed: 18620091]

Wang MH, Ronsin C, Gesnel MC, Coupey L, Skeel A, Leonard EJ, Breathnach R. Identification of the ron gene product as the receptor for the human macrophage stimulating protein. Science. 1994; 266:117–119. [PubMed: 7939629]

Wang MH, Yoshimura T, Skeel A, Leonard EJ. Proteolytic conversion of single chain precursor macrophage-stimulating protein to a biologically active heterodimer by contact enzymes of the coagulation cascade. J Biol Chem. 1994b; 269:3436–3440. [PubMed: 7508914]

Welm AL, Sneddon JB, Taylor C, Nuyten DS, van de Vijver MJ, Hasegawa BH, Bishop JM. The macrophage-stimulating protein pathway promotes metastasis in a mouse model for breast cancer and predicts poor prognosis in humans. Proc Natl Acad Sci U S A. 2007; 104:7570–7575. [PubMed: 17456594]

Wiseman BS, Werb Z. Stromal effects on mammary gland development and breast cancer. Science. 2002; 296:1046–1049. [PubMed: 12004111]

Zinser GM, Leonis MA, Toney K, Pathrose P, Thobe M, Kader SA, Peace BE, Beauman SR, Collins MH, Waltz SE. Mammary-specific Ron receptor overexpression induces highly metastatic mammary tumors associated with beta-catenin activation. Cancer Res. 2006; 66:11967–11974. [PubMed: 17178895]

Research Highlights

- HGFL is expressed in both the epithelial and stromal compartments of developing murine mammary glands.
- HGFL deficiency delays early postnatal mammary gland ductal elongation.
- HGFL deficiency alters epithelial cell turnover in the TEB throughout puberty by decreasing cell proliferation and increasing cell apoptosis.
- HGFL loss leads to decreased macrophage recruitment to the terminal end buds of the developing mammary gland.
- HGFL promotes the expression and activation of STAT3 during mammary gland development.

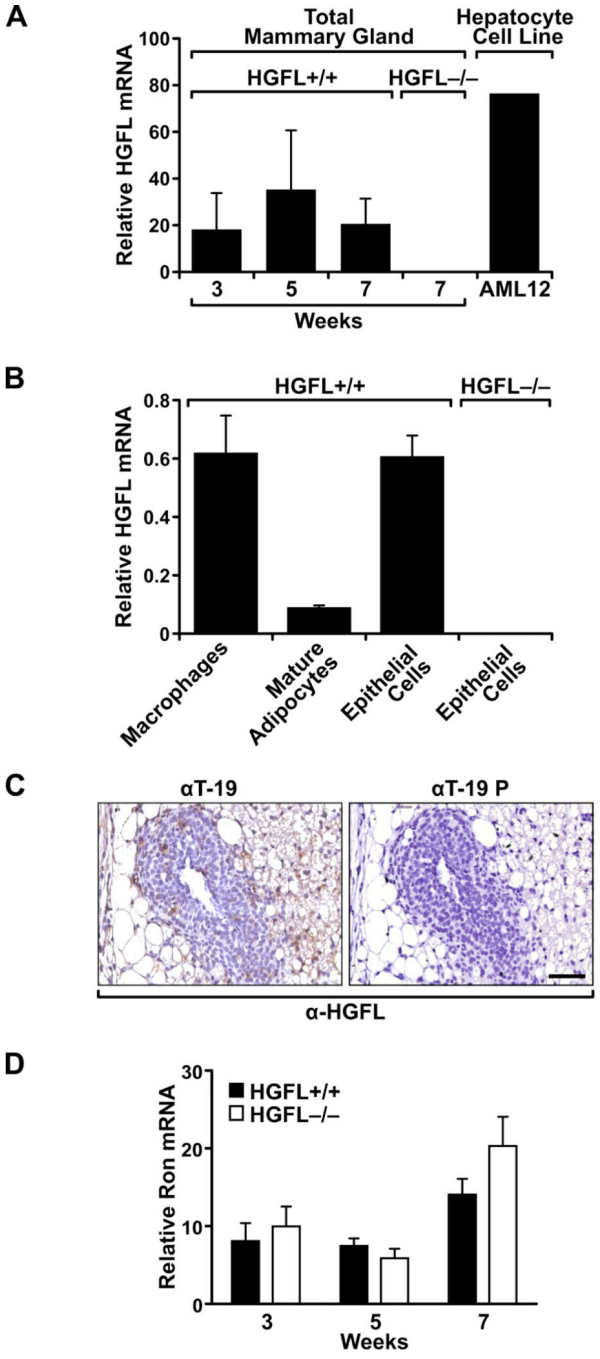

Figure 1. HGFL is expressed in both the epithelial and stromal cell compartments during mammary gland development

(A) qRT-PCR analysis for HGFL mRNA expression from 3, 5, and 7 week old HGFL+/+ virgin mouse mammary glands. Mammary glands from 7 week old HGFL−/− mice served as the negative control and the mouse hepatocyte cell line AML12 served as the positive control. Expression levels were normalized to mGUS as an internal control and the relative expression of HGFL mRNA is shown. (n=2–5 per group). **(B)** qRT-PCR analysis for HGFL mRNA expression using RNA isolated from epithelial, mature adipocyte, and macrophage

cell fractions from 5 week old HGFL+/+ mammary glands. RNA isolated from HGFL−/− purified epithelial cells was used as a negative control. Expression levels were normalized to mGUS and the relative expression of HGFL mRNA is shown. (n=2–4 per group). **(C)** Immunohistochemical detection of HGFL (αT-19) in 5-week-old HGFL+/+ mammary gland sections. HGFL positive cells stain brown. HGFL expression was localized to TEB epithelial cells and stromal cells surrounding the TEBs. Antibody specificity for HGFL was confirmed with the inclusion of a HGFL blocking peptide (αT-19 P) to the IHC. Scale bar=100μm. **(D)** qRT-PCR analysis for Ron mRNA expression using RNA isolated from 3, 5, and 7 week old age matched HGFL+/+ and HGFL−/− mammary glands. Expression levels were normalized to mGUS and relative expression of Ron mRNA is shown. (n=4–8 per group). Bars depict average values ± SEM.

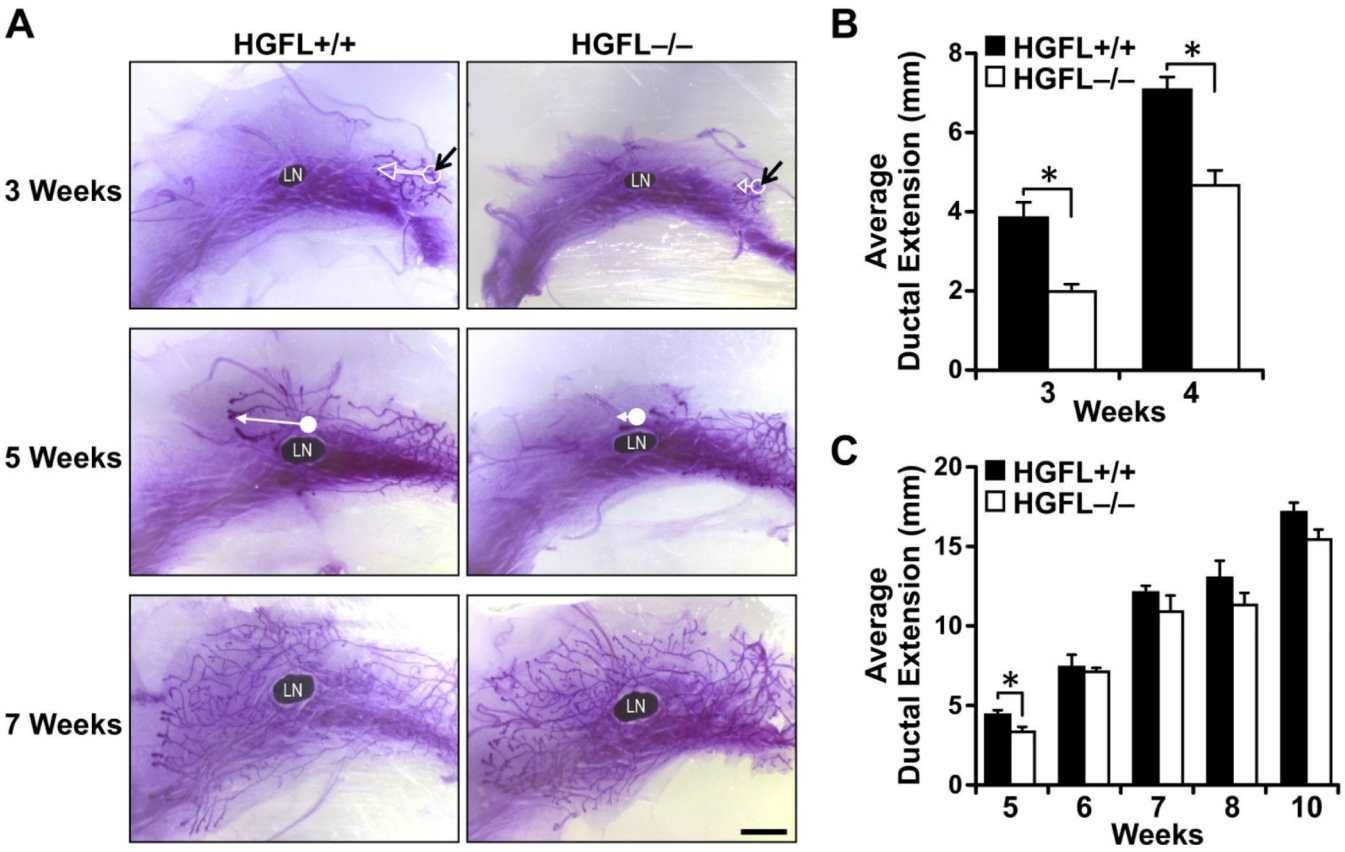

Figure 2. HGFL deficiency delays early postnatal mammary gland development

(A) Inguinal mammary glands isolated from age matched HGFL+/+ and HGFL−/− female mice at multiple developmental time points were examined by whole mount analysis. Images of representative whole mounts of HGFL+/+ and HGFL−/− inguinal mammary glands at 3, 5, and 7 weeks of age illustrate the mammary gland ductal network. Black arrows point to the nipple region of the rudimentary mammary gland at 3 weeks of age, while the white arrows show the parameters used for ductal extension measurements as described in the Materials and Methods section. Images illustrate the stunted epithelial penetration of the mammary fat pads in the HGFL−/− mammary glands in early puberty. The mammary lymph node (LN) is indicated for orientation. Scale bar=2mm. **(B and C)** Mammary gland ductal extension at multiple developmental time points was quantified as described in the Materials and Methods section and the histogram represents the average per group. Error bars represent ± SEM. *P<0.05 compared to the corresponding control group. (n=5–18 per group).

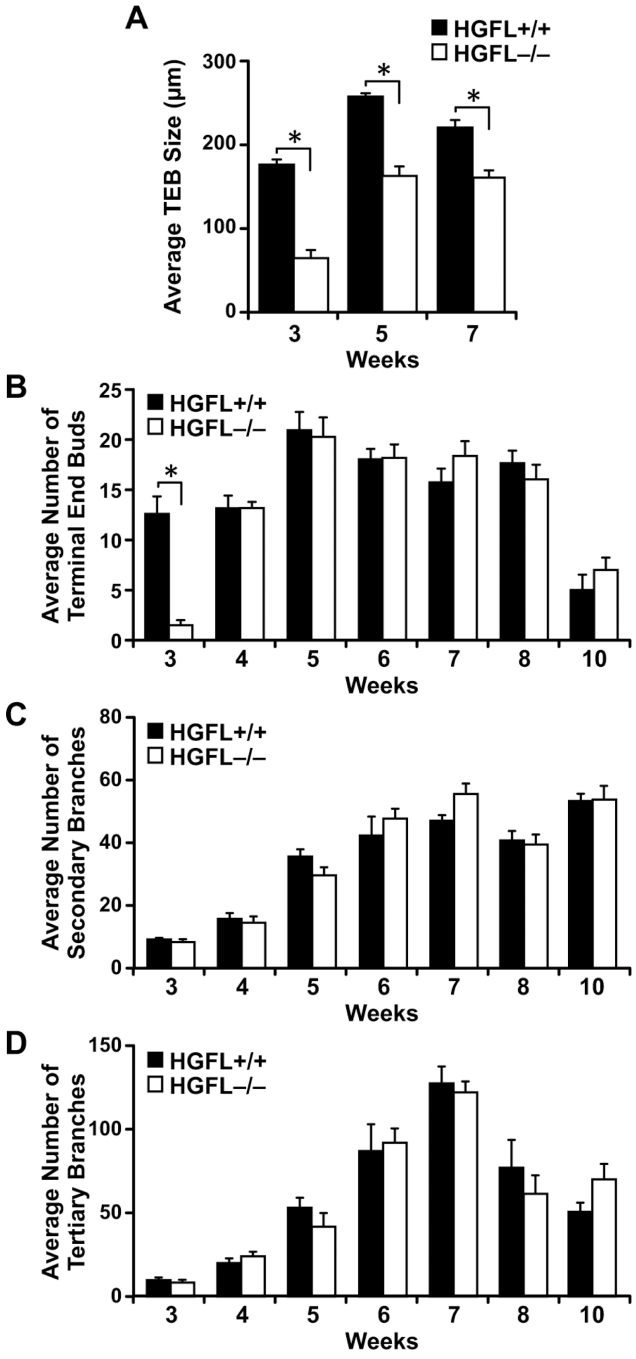

Figure 3. HGFL deficiency delays early postnatal mammary gland development

As described in the Materials and Methods section, the size of Terminal End Buds **(A)**, number of Terminal End Buds **(B)**, the number of secondary branches **(C)**, and the number of tertiary branches **(D)** were quantified and graphed as averages for each group. Error bars represent ± SEM. *P<0.05 compared to the corresponding control group. (n=3–16 per group).

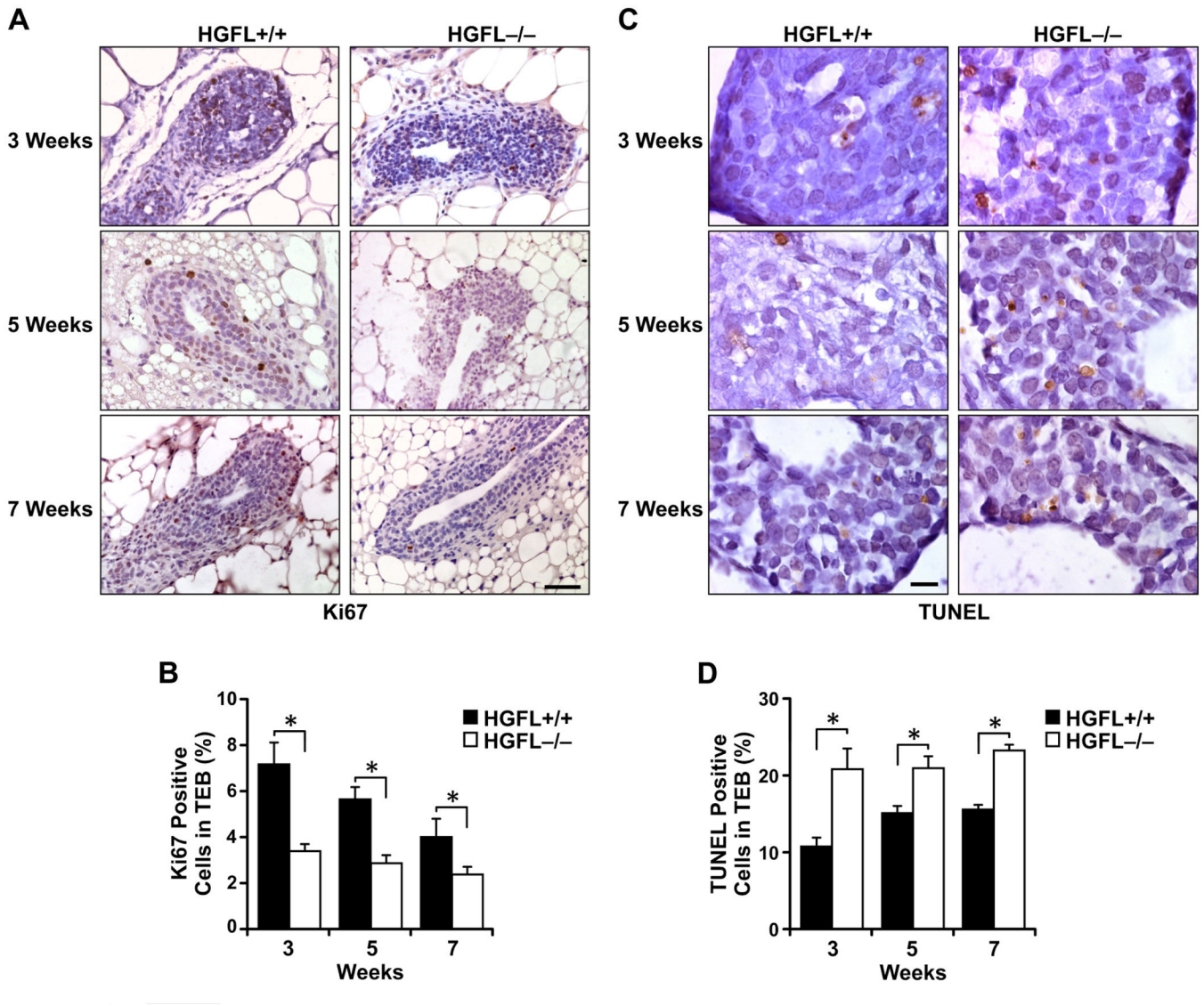

Figure 4. Epithelial cell turnover in the normal mammary gland depends on HGFL

(A) Immunohistochemical staining for Ki67 on 3, 5, and 7 week old age matched HGFL+/+ and HGFL−/− mammary gland sections. Brown staining in the TEBs represents the Ki67 positive cells. Scale bar = 100μm. (n=6–15 per group). **(B)** Quantification of the average percent of Ki67 positive cells in TEBs of HGFL+/+ and HGFL−/− mammary glands. **(C)** Immunohistochemical staining for TUNEL on 3, 5, and 7 week old age matched HGFL+/+ and HGFL−/− mammary gland sections. Brown staining in the TEBs represents the TUNEL positive cells. Scale bar=10μm. (n=3–5 per group). **(D)** Quantification of the average percent of TUNEL positive cells in the TEBs of HGFL+/+ and HGFL−/− mammary glands. (n=4–28 fields/TEBs from a minimum of 3 mice per group). Histograms represent the average per group ± SEM. *P<0.05 compared to the corresponding control group.

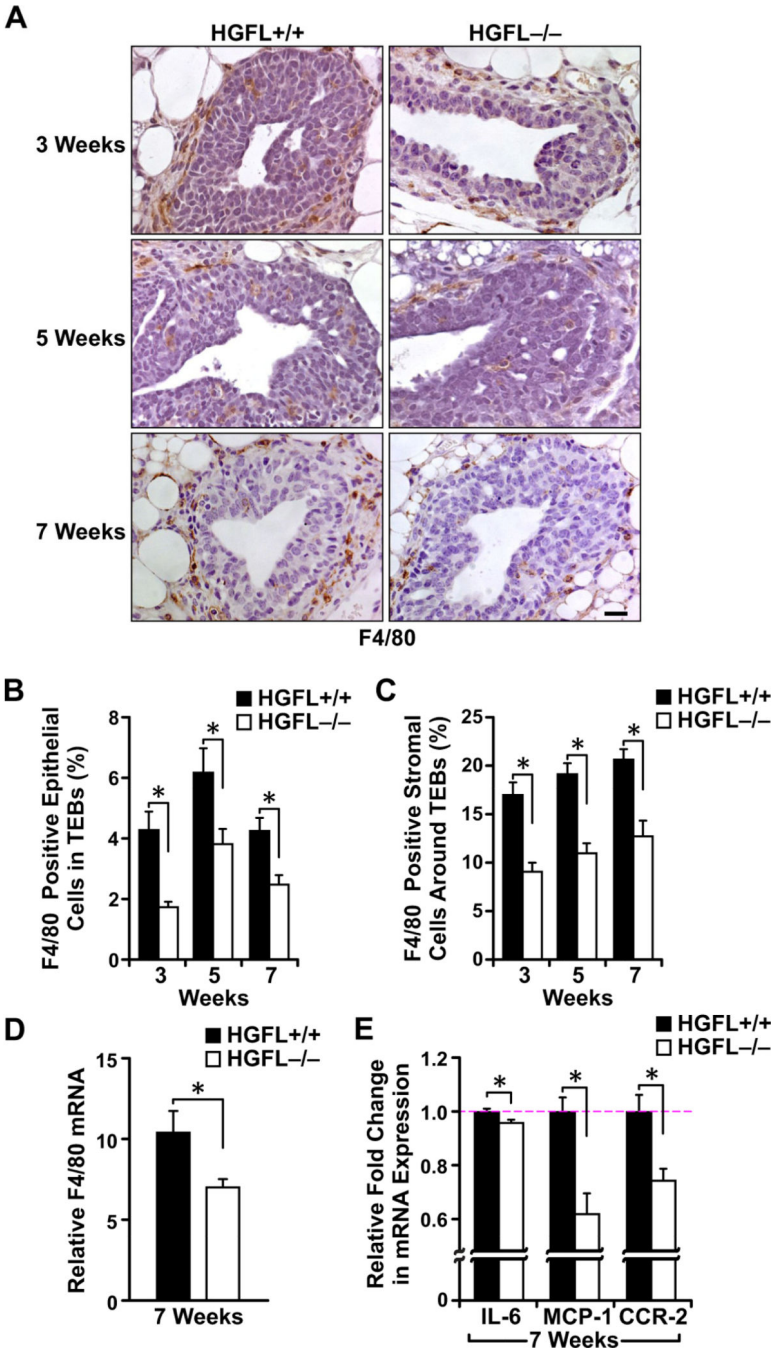

Figure 5. HGFL+/+ mammary glands have increased association of macrophages in both the epithelial and stromal areas surrounding the TEBs of the developing mammary gland

(A) Immunohistochemical staining for F4/80 on 3, 5, and 7 week old age matched HGFL+/+ and HGFL−/− mammary gland sections. Brown staining on the sections represents the F4/80 positive cells. Scale bar=20μm. (n=8–19 fields/TEBs with a minimum of 4 mice per group). **(B)** Quantification of the average percent of macrophages in the TEBs and **(C)** the average percent of macrophages in the stroma surrounding the TEBs in HGFL+/+ and HGFL−/− animals. **(D)** qRT-PCR analysis for F4/80 in 7 week old HGFL+/+ and HGFL−/− mammary glands. Expression levels were normalized to mGUS and relative expression of F4/80

mRNA is shown. (n=5–8 per group). **(E)** qRT-PCR analysis for IL-6, MCP-1, and CCR-2 in 7 week old HGFL+/+ and HGFL−/− mammary glands. Expression levels were normalized to mGUS and relative expression of IL-6, MCP-1, and CCR-2 mRNA is shown ± SEM. (n=4–13 per group). *P<0.05 compared to the corresponding control group.

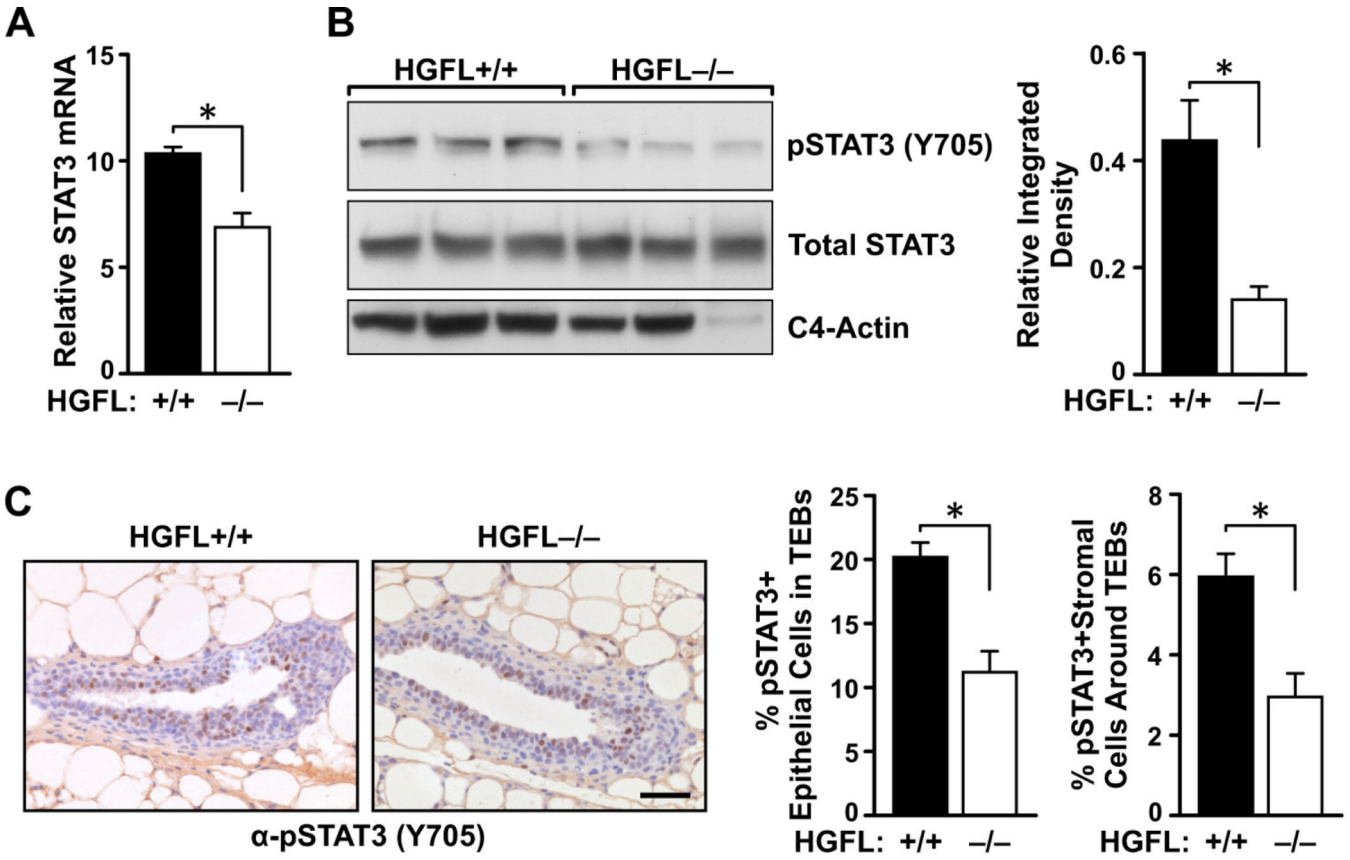

Figure 6. HGFL-mediated Ron signaling in the mammary gland is associated with increased STAT3 mRNA expression and protein phosphorylation

(A) qRT-PCR for STAT3 in 3 week old HGFL+/+ and HGFL−/− mammary glands. Expression levels were normalized to mGUS and relative expression of STAT3 mRNA is shown. (n=3 per group). **(B)** Western analyses for pSTAT3, total STAT3, and actin on 3 week old HGFL+/+ and HGFL−/− mammary glands. Each lane represents an individual mouse (n=3 per group). The right inset shows the relative densitometric quantification of pSTAT3 relative to total STAT3 from the immunoblotting analysis. **(C)** Immunohistochemical analysis of pSTAT3 localization using an anti-pSTAT3 antibody in 3 week old HGFL+/+ and HGFL−/−mammary gland sections. Brown staining in the TEBs as well as in the stromal region shows positive pSTAT3 staining. Scale bar=100μm. Right inset shows quantification of the average percent of pSTAT3 positive epithelial cells in the TEBs (left panel) and surrounding stromal cells (right panel) of HGFL+/+ and HGFL−/− mammary glands ± SEM. (n=7–25 fields/TEBs with a minimum of 5 mice per group). *P<0.05 compared to the control group.